Available online at www.sciencedirect.com
ScienceDirect
Talanta 74 (2008) 879–886
Talanta
www.elsevier.com/locate/talanta

Glucose biosensors based on platinum nanoparticles-deposited carbon nanotubes in sol–gel chitosan/silica hybrid

Xinhuang Kang [a,b], Zhibin Mai [a], Xiaoyong Zou [a,*], Peixiang Cai [a], Jinyuan Mo [a]

[a] *School of Chemistry and Chemical Engineering, Sun Yat-Sen University, Guangzhou 510275, PR China*
[b] *College of Science, Guangdong Ocean University, Zhanjiang 524088, PR China*

Received 31 May 2007; received in revised form 22 July 2007; accepted 23 July 2007
Available online 31 July 2007

Abstract

A new strategy for fabricating a sensitivity-enhanced glucose biosensor was presented, based on multi-walled carbon nanotubes (CNT), Pt nanoparticles (PtNP) and sol–gel of chitosan (CS)/silica organic–inorganic hybrid composite. PtNP-CS solution was synthesized through the reduction of $PtCl_6^{2-}$ by $NaBH_4$ at room temperature. Benefited from the amino groups of CS, a stable PtNP gel was obtained, and a CNT–PtNP–CS solution was prepared by dispersing CNT functionalized with carboxylic groups in PtNP–CS solution. The CS/silica hybrid sol–gel was produced by mixing methyltrimethoxysilane (MTOS) with the CNT–PtNP–CS solution. Then, with the immobilization of glucose oxidase (GOD) into the sol–gel, the glucose biosensor of GOD–CNT–PtNP–CS–MTOS–GCE was fabricated. The properties of resulting glucose biosensor were measured by electrochemical impedance spectroscopy (EIS) and cyclic voltammetry (CV). In phosphate buffer solutions (PBS, pH 6.8), nearly interference free determination of glucose was realized at low applied potential of 0.1 V, with a wide linear range of 1.2×10^{-6} to 6.0×10^{-3} M, low detection limit of 3.0×10^{-7} M, high sensitivity of 2.08 μA mM^{-1}, and a fast response time (within 5 s). The results showed that the biosensor provided the high synergistic electrocatalytic action, and exhibited good reproducibility, long-term stability. Subsequently, the novel biosensor was applied for the determination of glucose in human serum sample, and good recovery was obtained (in the range of 95–104%).

Keywords: Glucose; Biosensors; Carbon nanotubes; Platinum nanoparticles; Sol–gel; Chitosan

1. Introduction

Since Clark and Lyons [1] reported their enzyme electrode for measuring glucose, great attention has been devoted to glucose biosensors [2–6]. It is important to develop the methods with high sensitivity, good reproducibility, fast response, and easy fabrication for the determination of glucose in both clinical diagnostics and food industry analysis. In recent years, nanomaterials, such as carbon nanotubes (CNT) and metal nanoparticles, have been widely applied to biosensors. CNT have good performances of high surface-to-volume ratios and fast electron-transfer kinetic for a wide range of electroactive species in the construction of biosensor [7–12]. Metal nanoparticles can display following unique advantages over macroelectrodes when used for electroanalysis: enhancement of mass transport, catalysis, high effective surface area and control over electrode microenviroment [13]. For example, Pt and Au nanoparticles are very effective as a matrix of enzyme sensors by taking advantage of the biocompatibility and huge surface [14,15]. Most work has been carried out using transition metal nanoparticles for biosensors, such as platinum [3], copper [4], silver [16] palladium [17], and gold [18]. Recently, there are some interesting researches on integrating nanoparticles with CNT to fabricate biosensors and easily to gain synergistic action with the hybrid of nanomaterials. The methods of nanohybridization are completed by solvent DMF [19], polymers, such as CS [20–22], Nafion [23–26], and an appropriate surfactant dihexadecyl hydrogen phosphate (DHP) [27]. The used techniques included sol–gel [3] process, metal nanoparticles self-assembly [28–31] and electrodeposition on the surface of CNT from metal salt solutions [32–35].

The immobilization of enzymes is a key step for the fabrication of biosensors. The common methods for immobilizing enzymes on electrodes include entrapment techniques [3], elec-

* Corresponding author. Fax: +86 20 84112455.
E-mail address: ceszxy@mail.sysu.edu.cn (X. Zou).

0039-9140/$ – see front matter © 2007 Elsevier B.V. All rights reserved.
doi:10.1016/j.talanta.2007.07.019

trochemical copolymerization [36], covalent or cross-linking [24], and adsorption [32]. Lately, sol–gel-derived materials have been applied for the immobilization of biomolecules to improve the performance of the biosensor [2,3,9,37,38]. The biosensor fabricated by this method possesses several advantages, such as high stability, wide potential window, and easy fabrication at room temperature and encapsulation for electrocatalysts and biocatalysts. Furthermore, porous and open frameworks of sol–gel ensure that the analytes can effectively and fast access to the active functionalities immobilized at the interface between electrode and solution, which results in a high sensitivity to the electrochemical response, as most electron transfer processes are diffusion-controlled. However, the silica sol–gel, which is common used, is brittle and low biocompatible. In order to overcome these obstacles, silica-based organic–inorganic hybrids are adopted as attractive composite materials for the fabrication of biosensors [39]. Some polymers are hybridized into a silica sol–gel matrix, such as polyhydroxyle (PVA–g–PVP) [2], CS [9,40], poly(vinyl alcohol)(PVA) [41], which can effectively avoid the brittleness of pure inorganic sol–gel and the swelling of some pure polymers.

In this work, a new glucose biosensor was developed, based on the signal-enhanced effect of CNT, PtNP and sol–gel of CS/silica organic–inorganic hybrid composite film. The properties of resulting glucose biosensor were characterized by EIS and CV. The resulting biosensor exhibited several advantages, such as high sensitivity at a low potential, good stability, and easy fabrication at room temperature and encapsulation for nanomaterials and biocatalysts. Furthermore, the biosensor was applied for the determination of glucose in human serum sample.

2. Experimental

2.1. Materials and apparatus

CNT (∼95% purity) were purchased from Shenzhen Nanotech Port Co. (China). Glucose oxidase (EC1.1.3.4, 195,000 unit g^{-1}) was obtained from Sigma. CS (90% deacetylated, MW $\sim 1 \times 10^6$) was bought from Shanghai Biochemical (China). Methyltrimethoxysilane (MTOS) was purchased from Aldrich. D-Glucose and H_2PtCl_6 were obtained from Guangzhou Chemical reagent company (China). PBS (20 mM KH_2PO_4 + 20 mM K_2HPO_4 + 0.1 M KCl, pH 6.8) was used as supporting electrolyte. A stock solution of D-glucose (0.1 M) was allowed to mutarotate at room temperature for 24 h before use.

The electrochemical experiments were performed with CHI660A electrochemical workstation (China). All experiments were carried out by three-electrode system with a glassy carbon electrode (GCE, $\Phi = 3$ mm) as the working electrode, a platinum wire as the auxiliary electrode, and an Ag/AgCl/3.0 M KCl as the reference electrode. JEM-2010 transmission electron microscope (TEM; Japan) was operated for the TEM experiment at an accelerating voltage of 200 kV. JSM-6330F scan electron microscopy (SEM; Japan) was applied for the SEM experiment. X-Ray diffraction (XRD) data of the sample was recorded on a Rigaku D/max 2200vpc diffractometer (Japan) using Cu Kα1 radiation ($\lambda = 0.154056$ nm) with a Ni filter.

2.2. Preparation of the modified electrodes

PtNP–CS solution was prepared according to the literature [20,42]. Briefly, CS solution was mixed with H_2PtCl_6, and then the reduction of $PtCl_6^{2-}$ by $NaBH_4$ yielded a clear black colored solution, which was designated as 100% PtNP stock solution. The other stock solutions were prepared by dispersing 2.0 mg CNT functionalized with carboxylic groups in 1.0 mL 0.2% CS solution or PtNP–CS solution. The sol–gel of CNT–PtNP–CS–MTOS was prepared by mixing 10 μL MTOS, 20 μL ethanol, and 1.0 mL CNT–PtNP–CS solution in a 2.0 mL PVC tube [9]. The mixture was sonicated for 10 min, and then stored at room temperature for 3 h. 10.4 mg GOD was dissolved in 1.0 mL PBS as a stock solution (2 U μL^{-1}), and stored at 4 °C. Fifty microliter CNT–PtNP–CS–MTOS sol–gel and 50 μL GOD solution were mixed in a 0.5 mL PVC tube. GOD–CNT–PtNP–CS–MTOS–GCE biosensor was fabricated after 8 μL of the mixture was dropped on the surface of GCE and dried at 4 °C in a refrigerator for 24 h. All the enzyme modified electrodes were stored at 4 °C in the dry state.

3. Results and discussion

3.1. Physical characterization of PtNP–CS and PtNP–CNT–CS–MTOS

TEM image (Fig. 1A) showed PtNP was well dispersed in the CS solution. The size of particles was observed around 3–4 nm, which illustrated that amino groups played an important role in the stabilization of PtNP in CS solution. No aggregation of the nanoparticles was noticed after 2 months. When CNT functionalized with carboxylic groups and MTOS were added and sonicated, the nanohybrid and sol–gel were formed. Fig. 1B depicted PtNP and CNT were dispersed in sol–gel. XRD spectrum of PtNP–CS composite was illustrated in Fig. 1C. The diffraction pattern clearly indicated there were three major peaks at 39.6°, 46.1° and 67.2°, which can be assigned to (1 1 1), (2 0 0), and (2 2 0) planes of the face-centered cubic lattice of Pt(0), respectively. Based on Scherrer formula [43], $L = 0.9\,\lambda_{Ka1}/B_{(2\theta)}\cos\theta_B$, where L is the average size of particles, λ_{ka1} the X-ray wavelength, $B_{(2\theta)}$ the peak broadening, and θ_B is the angle of the peak maximum. From the experimental result, L value of 4.1 nm was calculated, which is in good agreement with the result from the TEM image.

Robust and uniform CS membranes were easily formed at room temperature by evaporating water from CS solution, due to hydrogen bonds between hydroxy and amino groups. CS was hybridized with MTOS to improve the permeability of CS and to utilize the advantages of organic–inorganic hybrid materials. The hybrid film has good performance for the biosensor, when the ratio of MTOS and CS was 1:1 [9]. The SEM images showed that the CS–MTOS hybrid film was porous and open framework (Fig. 1D), and it was uniformity with GOD (Fig. 1E).

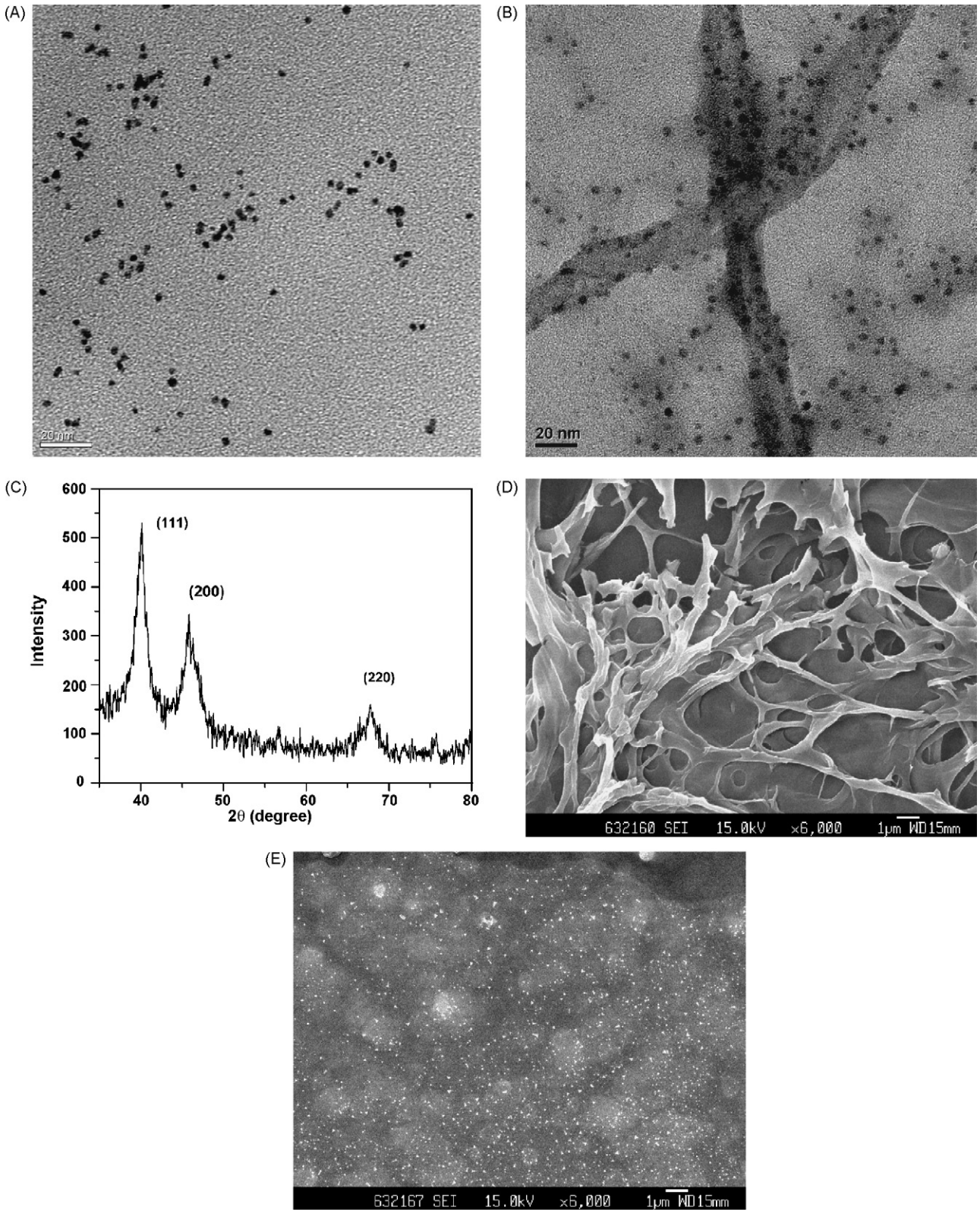

Fig. 1. TEM images of PtNP–CS solution (A) and CNT–PtNP–CS–MTOS sol–gel (B); XRD pattern of PtNP–CS composite (C); SEM images of the hybrid film of MTOS–CS (D) and GOD–MTOS–CS (E).

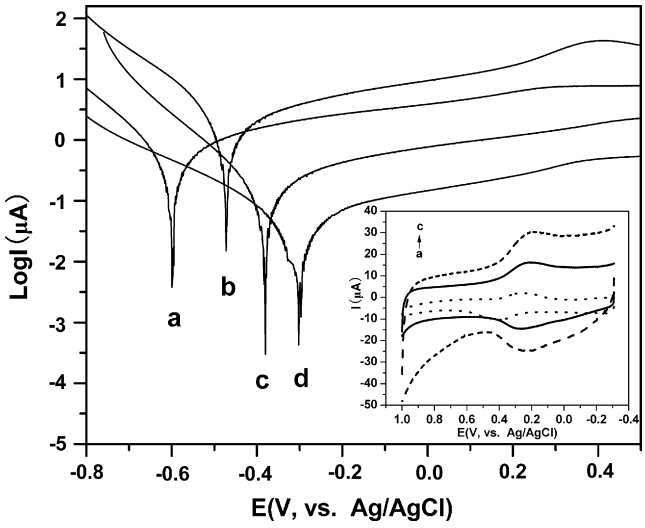

Fig. 2. (A) Polarization curves for unmodified and modified GCEs: (a–d) CNT–CS–MTOS–GCE, CNT–PtNP–CS–MTOS–GCE, PtNP–CS–MTOS–GCE, GCE in 0.5 M H_2SO_4 at 10 mV s^{-1}. Inset: CVs in 0.5 M H_2SO_4 at 50 mV s^{-1}: (a–c) PtNP–CS–MTOS–GCE, CNT–CS–MTOS–GCE, CNT–PtNP–CS–MTOS–GCE.

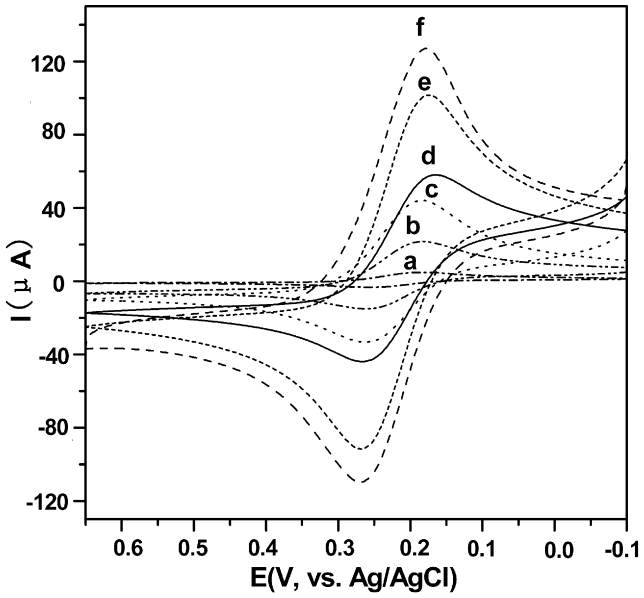

Fig. 3. CVs of unmodified and modified GCEs in 20 mM $[Fe(CN)_6]^{4-}$ with 0.2 M KCl at 20 mV s^{-1}: (a–f) CS–GCE, CS–MTOS–GCE, PtNP–CS–MTOS–GCE, CNT–CS–MTOS–GCE, GCE, CNT–PtNP–CS–MTOS–GCE.

3.2. Electrochemical characterization of the modified electrodes

Linear sweep voltammetry (LSV) was conducted for four different types of electrodes: bare GCE, CNT–CS–MTOS–GCE, PtNP–CS–MTOS–GCE and CNT–PtNP–CS–MTOS–GCE. The CNT–CS–MTOS–GCE provoked a negative shift of corrosion potential (E_{corr}) from −0.31 V of the bare GCE (Fig. 2d) to −0.60 V (Fig. 2a), due to the specific electrochemical properties of CNT. The E_{corr} of the PtNP–CS–MTOS–GCE (Fig. 2c) shifted from −0.31 V of the bare GCE to −0.38 V. The E_{corr} of the CNT–PtNP–CS–MTOS–GCE (Fig. 2b) shifted in the opposite direction from −0.60 to −0.47 V, which was ascribed to the more noble electrochemical characteristics of platinum. The variety of less negative values of potentials clearly showed that PtNP hybrid in sol–gel revealed higher stability of the CNT–PtNP–CS–MTOS–GCE. The CV (Fig. 2 inset c) indicated a high electrocatalytic activity for the oxygen reduction between −0.20 and + 0.40 V, which was in accordance with the literature [20]. Smaller currents to O_2 reduction were observed (Fig. 2 inset a and b) for the PtNP–CS–MTOS–GCE and CNT–CS–MTOS–GCE, respectively.

Fig. 3 showed the CVs of bare GCE and the modified electrodes in 20 mM $[Fe(CN)_6]^{4-}$ with 0.2 M KCl at 20 mV s^{-1}. Quasi-reversible one-electron redox behavior of ferricyanide ion was observed on the bare GCE (Fig. 3e) with a peak separation (ΔE_p) of 70 mV. After the electrode was modified with CS, the lower peak current (I_p) and larger ΔE_p were observed (Fig. 3a), due to the CS membrane hindering the diffusion of ferricyanide ion towards the GCE surface. For CS–MTOS–GCE (Fig. 3b), I_p increased in comparison with that of the CS–GCE, because of the sol–gel hybrid with porous and open frameworks. It was illustrated in Fig. 3c that larger I_p and smaller ΔE_p were observed for PtNP–CS–MTOS–GCE compared with CS–MTOS–GCE, which indicated that PtNP played a role in the increase of the electroactive surface area. Fig. 3d showed the voltammetric response of ferricyanide ion on the CNT–CS–MTOS–GCE because CNT have a very high catalytic active surface and aspect ratio. For CNT–PtNP–CS–MTOS–GCE (Fig. 3f), I_p was the highest among the electrodes. The results confirmed that the CNT–PtNP–CS–MTOS composite film, which was effectively immobilized on the GCE surface, can provide the necessary conduction pathways, and promote the electron transfer of analyte between the interface of solution and electrode. It also indicated the largest electroactive surface area, according to the Randles–Sevcik equation ($I_p = 2.69 \times 10^5 AD^{1/2} n^{3/2} \nu^{1/2} C$) [44]. The average value of the electroactive surface area for CNT–PtNP–CS–MTOS–GCE (1.0 mg/mL CNT in 100% PtNP sol–gel) was $(7.67 \pm 0.20) \times 10^{-2}$ cm^2 ($n = 6$), compared with $(7.07 \pm 0.10) \times 10^{-2}$ cm^2 ($n = 6$) for bare GCE.

EIS can provide information on the impedance changes of the electrode surface during the modification process. The electron-transfer resistance (R_{ct}) at the electrode surface is equal to the semicircle diameter. Fig. 4 presented the Nyquist plots of the impedance spectroscopy of the bare GCE and modified electrodes. The R_{ct} of CS film (Fig. 4g, 1050 Ω) was much larger than that of bare GCE (Fig. 4b, 180 Ω), which indicated that a film of CS was formed on the electrode surface, and could block the electron transfer of $[Fe(CN)_6]^{3-/4-}$ in some degree. For the porous film of MTOS–CS (Fig. 4f), R_{ct} decreased to 800 Ω compared with that of the CS film, because the electron transfer became easy between the solution and the electrode. After the films of PtNP–CS–MTOS and CNT–CS–MTOS were formed, R_{ct} decreased to about 520 and 400 Ω, respectively (Fig. 4e and d). When the film of CNT–PtNP–CS–MTOS was formed, R_{ct} was the lowest around 150 Ω (Fig. 4a), which was in accordance with the fact that the film of sol–gel integrated PtNP with CNT enhanced the synergistic electrocatalytic activity. The results

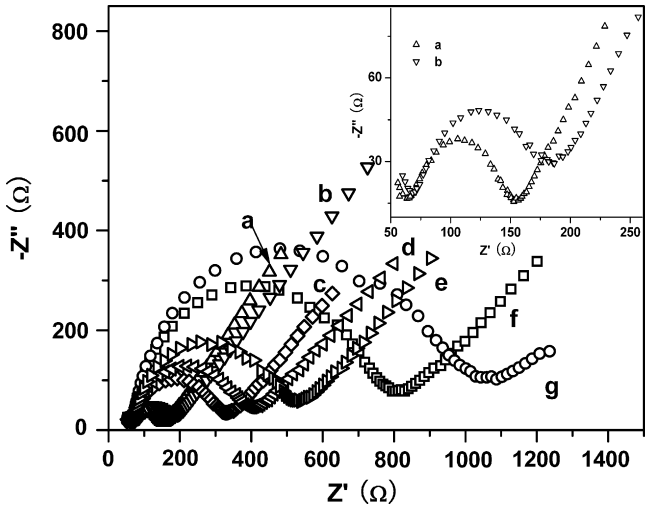

Fig. 4. Nyquist plots of EIS for: (a–g) CNT–PtNP–CS–MTOS–GCE, GCE, GOD–CNT–PtNP–CS–MTOS–GCE, CNT–CS–MTOS–GCE, PtNP–CS–MTOS–GCE, MTOS–CS–GCE, CS–GCE, inset: magnified of (a and b). Supporting electrolyte was 10 mM $[Fe(CN)_6]^{3-/4-}$ with 0.1 M KCl. The applied potential was 0.16 V.

were in agreement with CV (Fig. 3). However, R_{ct} increased to 340 Ω (Fig. 4c) by immobilizing the GOD onto the CS–MTOS.

3.3. Electrochemical performance of the glucose biosensor

CVs were shown in Fig. 5 for bare GCE and modified with CNT–PtNP–CS–MTOS in PBS without and with 0.1 mM H_2O_2. For the GCE modified with CNT–PtNP–CS–MTOS, the current signal to H_2O_2 (Fig. 5d) is higher than that of the bare GCE (Fig. 5b). The excellent electrocatalytic activity of the electrode to H_2O_2 made it attractive for the fabrication of biosensor, as H_2O_2 is a product of a number of oxidase-based enzyme reactions. Glucose oxidase was selected as a model enzyme. Many glucose biosensors are based on GOD, which catalyzes the oxidation of glucose to gluconolactone and hydrogen peroxide:

$$\text{Glucose} + O_2 \rightarrow H_2O_2 + \text{Gluconolactone}$$

The GOD–NT–tNP–CS–MTOS–GCE was formed by immobilizing GOD on the electrode surface through sol–gel of CS/silica organic–inorganic hybrid with CNT and PtNP.

The effect of pH and the amount of enzyme loaded in the composite on the response current of the biosensor was investigated (Fig. 6A). Maximum response current was obtained at pH 6.8, when 12 unit GOD was applied for the determination of 0.5 mM glucose at 0.4 V. Fig. 6B depicted that the current signals increased with the varying content of CNT from 0.2 to 1.0 mg mL^{-1}, due to the increase of electroactive material in the composite. No changes of the response current were

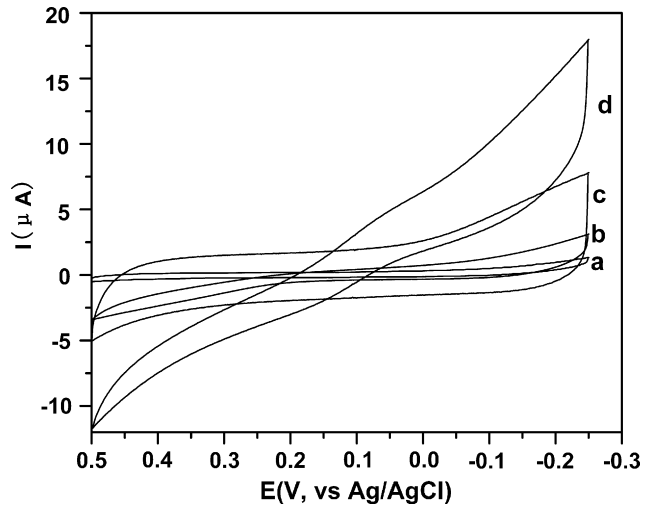

Fig. 5. CVs of GCE (a, b) and CNT-PtNP-CS-MTOS-GCE (c, d) in PBS at 50 mV s^{-1} in the absence (a, c) and presence (b, d) of 0.1 mM H_2O_2.

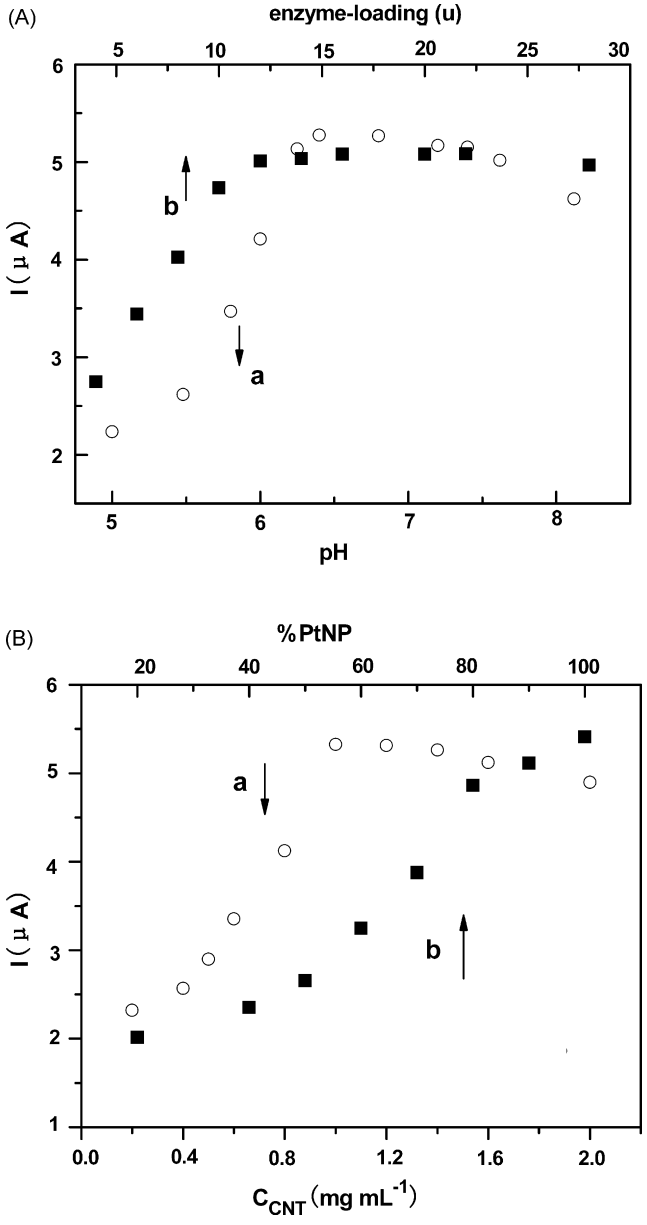

Fig. 6. (A) Effect of pH (a) and enzyme loading (b); (B) effect of CNT (a) and %PtNP concentration (b) for GOD–CNT–PtNP–MTOS–CS–GCE on current response of 0.5 mM glucose at 0.4 V.

noticed when the loading amount of CNT exceeded 1 mg mL^{-1}, which may be attributed to the poor dispersant of CNT in sol–gel and the leakage of CNT from the film of the modified electrode. With fixed CNT content of 1 mg mL^{-1}, the current response obviously increased by varying PtNP–CS from 20% to 100%. Consequently, the CNT content of 1 mg mL^{-1} and 100% PtNP–CS in the stock solution were selected to modify the electrodes.

The electrocatalytic activity of GOD–CNT–PtNP–MTOS–CS–GCE to glucose was also investigated. Fig. 7A showed the response currents to 0.2 mM glucose at various applied potential from 0.0 to 0.6 V. At 0.2 V, the observed response current was insignificant. However, the cathodic response current increased at 0.0 and 0.1 V. While varying the applied potential from 0.3 to 0.6 V, the anodic response currents increased, in addition, the response time was very fast (within 5 s). The results can be attributed to the fast diffusion of glucose in the hybrid film, the fast electrons transfer for the integration of PtNP with CNT, and the fast chemical reaction equilibrium. Fig. 7A indicated that the fabricated biosensor has a flexible operating potential range for the monitoring of the oxidation/reduction of H_2O_2 that is a product of the oxidase-based GOD reaction. And by choos-

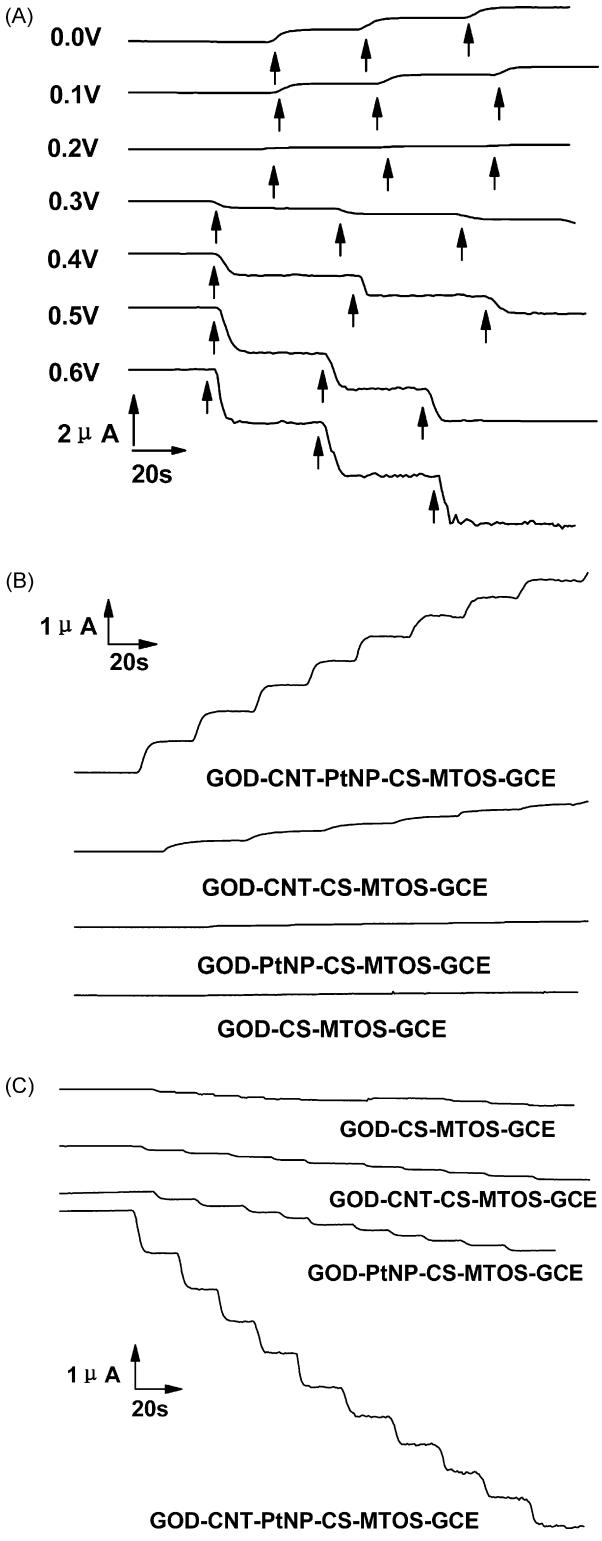

Fig. 7. Current response of GOD–CNT–PtNP–CS–MTOS–GCE at various applied potential (A) and different modified electrodes to 0.2 mM glucose in PBS at 0.1 V (B), 0.4 V (C).

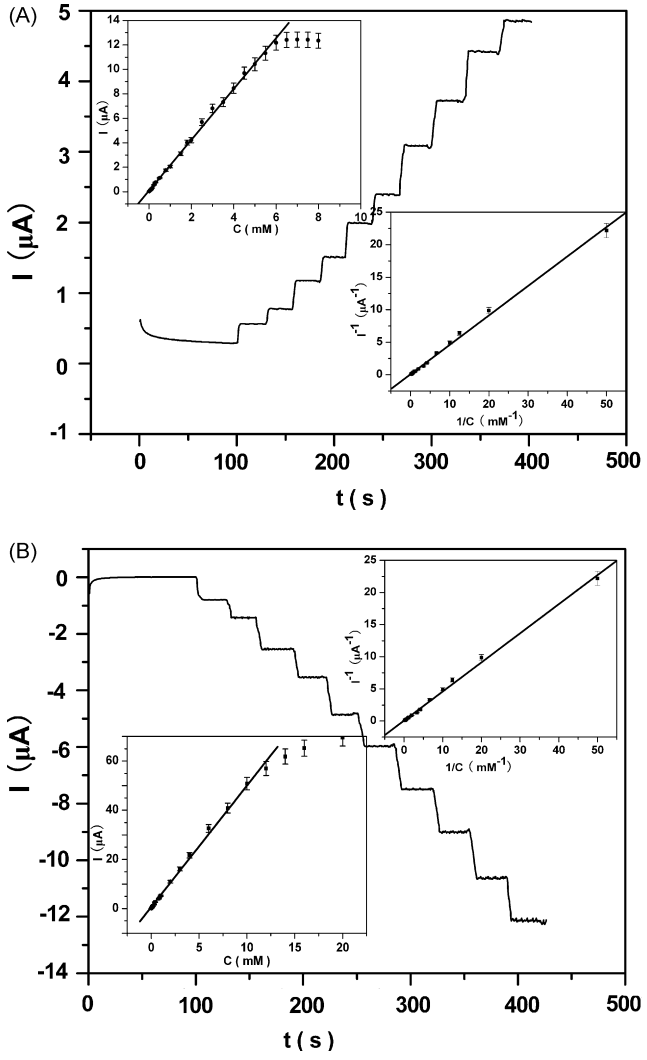

Fig. 8. Current response of GOD–CNT–PtNP–CS–MTOS–GCE to various concentrations of glucose at 0.1 V (A) and 0.4 V (B); Calibration curves and Lineweaver–Burk plots of the biosensor at 0.1 V (A inset left, right) and 0.4 V (B inset right, left).

Table 1
Summary on the performance of various CNT–PtNP-based glucose biosensors

Fabrication of biosensors	Sensitivity ($\mu A\,mM^{-1}$)	Linear range (mM)	Response Time (s)	Applied potential (V)	K_m^{app} (mM)
GOD/PtNP/CNT/Carbon paste [3]	–	0.1–35	<10	0.6	–
	0.28	1–25	<15	0.1	–
GOD/PtNP–CNT–Nafion/GCE [24]	2.11	0.0005–5	3	0.55	–
GOD/Nafion/PtNP/CNT/GCE [26]	0.64	0.02–4	<5	0.5	–
Nafion/GOD/PtNP/ACNT [30]	–	0.01–7	<5	0.3	9.28
(Pt-DENs/GOD)$_4$/CNT/Pt electode [31]	0.96	0.005–0.65	<5	0.0	–
Nafion/GOD/PtNP/CNT/Graphite [32]	14.5	0.1–13.5	<5	0.6	10.11
GOD–CNT–PtNP–CS–MTOS/GCE	2.08	0.0012–6	<5	0.1	5.8
(This work)	4.94	0.002–12	<5	0.4	7.9

Table 2
Determination of glucose in blood serums ($n = 6$)

Sample	Hospital (mM)	Biosensor (mM)	Relative error (%)	R.S.D. (%)	Added (mM)	Recovery (%)
1	5.5	5.4	−1.8	2.8	0.5	104
2	5.0	5.2	+4.0	3.2	0.5	98
3	5.2	5.0	−4.0	2.6	0.5	95
4	6.0	6.2	−3.3	2.8	0.5	102
5	4.2	4.5	+7.1	4.4	0.5	96
6	4.1	4.2	+2.4	3.0	0.5	104

ing the appropriate operating potential, commonly encountered electroactive interferences can be selectively avoided. At the applied potential of 0.1 and 0.4 V, the response current to glucose of the four types of modified electrodes were illustrated in Fig. 7B and C, respectively. The observed response current can be ignored for the GOD–CS–MTOS–GCE, and small response currents were noticed for GOD–PtNP–CS–MTOS–GCE and GOD–CNT–CS–MTOS–GCE. However, the response current for GOD–CNT–PtNP–CS–MTOS–GCE was the largest, which may be caused by the synergistic electrocatalytic action with the combination of PtNP and CNT.

Fig. 8 illustrated current-time plots for the biosensor on successive step changes of glucose concentration at the applied potential of 0.1 V (A) and 0.4 V (B), respectively. The calibration curves for the biosensor under the optimized experimental conditions were shown in Fig. 8A (left inset) and Fig. 8B (right inset). At 0.1 V, the biosensor displayed a linear range (1.2×10^{-6} to 6.0×10^{-3} M glucose) with a correlation coefficient of 0.9989, a sensitivity of 2.08 $\mu A\,mM^{-1}$, and the detection limit of 3.0×10^{-7} M at a S/N ratio of 3. At 0.4 V, it had a linear range from 2.0×10^{-6} to 1.2×10^{-2} M of glucose with a correlation coefficient of 0.9982, a sensitivity of 4.94 $\mu A\,mM^{-1}$, and the detection limit of 4.0×10^{-7} M when S/N is 3. The apparent Michaelis–Menten constant (K_m^{app}) was 5.8 mM (0.1 V) and 7.9 mM (0.4 V), respectively, according to the Lineweaver–Burk equation [45] from Fig. 8A (right inset) and Fig. 8B (left inset). These values were compared with those of the reported results of CNT–PtNP–based glucose biosensors (Table 1). The results confirmed that the biosensor had the good performances of high sensitivity, wide linear range, fast response, low applied potential, and small K_m^{app}, due to the enhancement of electroactive surface area and the synergistic electrocatalytic activity by combining PtNP with CNT, together with the use of biocompatible sol–gel of CS/silica organic–inorganic hybrid with porous and open framework.

The fabrication reproducibility of six GOD–CNT–PtNP–CS–MTOS modified electrodes was investigated by detecting 0.3 mM glucose at 0.4 and 0.1 V. The R.S.D.s were 5.2% and 5.5%, respectively. The storage stability of the biosensor was examined over 30-day-period for the response to 0.3 mM glucose at 0.1 V. After 30 days of storage at 4 °C, the response current was still retained above 80% of the initial response, which indicated the biosensor had a good reproducibility and stability. The interferences, such as ascorbic acid, uric acid, and lactic acid, are common problems in the electrochemical determination of glucose in physiological samples. At 0.4 V, the biosensor response was significantly affected by the acids at 0.1 mM level, the response signals of the acids were nearly eliminated at the potential of 0.1 V. At 0.1 V, the ratio of I_{G+I} to I_G was 1.007, 1.002 and 1.001 of ascorbic acid, uric acid, and lactic acid, respectively, where I_G is the response current to 0.5 mM glucose and I_{G+I} is the response to 0.5 mM glucose in the presence of interferences at 0.1 mM content.

The application of the biosensor was assessed by the determination of glucose concentration in human serum. 0.2 mL serum was added into 5.0 mL PBS, and the response current was obtained at 0.1 V. The results (Table 2) were in agreement with those detected by the hospital (human serum samples and spectrometric results were supplied by the first hospital attached to Sun Yat-Sen University).

4. Conclusions

In this paper, a new composite biosensor was constructed by integrating PtNP with CNT in the sol–gel of CS/silica organic–inorganic hybrid. CS with amino and hydroxy groups

can stabilize PtNP, disperse CNT, and form organic–inorganic hybrid sol–gel with MTOS. Consequently, the synergistic electrocatalytic action can be easily obtained by the integration of PtNP with CNT. With the immobilization of GOD, the glucose biosensor has the characteristics of high sensitivity, good reproducibility and stability, together with low applied potential, fast response, and free interferences. Other enzyme may be immobilized to construct useful biosensors for the detection of other target analytes. It is also possible to fabricate microbiosensors with this technique for the on-line spot detection.

Acknowledgements

This work was supported by the NNSF of China (No. 20475068, 20575082), the Natural Science Foundation of Guangdong Province (No. 031577, 7003714) and the Scientific Technology Project of Guangdong Province (No. 2005B30101003).

References

[1] L.C. Clark, J.C. Lyons, Ann. N. Y. Acad. Sci. 102 (1962) 29–45.
[2] B. Wang, B. Li, Q. Deng, S. Dong, Anal. Chem. 70 (1998) 3170–3174.
[3] M.H. Yang, Y.H. Yang, Y.L. Liu, G.L. Shen, R.Q. Yu, Biosens. Bioelectron. 21 (2006) 1125–1131.
[4] Q. Xu, Y. Zhao, J.Z. Xu, J.J. Zhu, Sens. Actuators B 114 (2006) 379–386.
[5] M. Zhao, A. Smith, W. Gorski, Anal. Chem. 76 (2004) 5045–5050.
[6] P.A. Fiorito, C.M.A. Brett, S.I.C. de Torresi, Talanta 69 (2006) 403–408.
[7] P.P. Joshi, S.A. Merchant, Y. Wang, D.W. Schmidtke, Anal. Chem. 77 (2005) 3183–3188.
[8] A. Merkoci, M. Pumera, X. Llopis, B. Perez, M. del Valle, S. Alegret, Tre. Anal. Chem. 24 (2005) 826–838.
[9] X.C. Tan, M.J. Li, P.X. Cai, L.J. Luo, X.Y. Zou, Anal. Biochem. 337 (2005) 111–120.
[10] J. Wang, M. Musameh, Y. Lin, J. Am. Chem. Soc. 125 (2003) 2408–2409.
[11] Q. Zhao, Z.H. Gan, Q.K. Zhuang, Electroanalysis 14 (2002) 1609–1613.
[12] L. Qian, X. Yang, Talanta 68 (2006) 721–727.
[13] C.M. Welch, R.G. Compton, Anal. Bioanal. Chem. 384 (2006) 601–619.
[14] Y. Ikariyama, S. Yamauchi, T. Yukiashi, H. Ushioda, Anal. Lett. 20 (1987) 1791–1801.
[15] S. Zhang, N. Wang, H. Yu, Y. Niu, C. Sun, Bioelectrochemistry 67 (2005) 15–22.
[16] X. Ren, X. Meng, D. Chen, F. Tang, J. Jiao, Biosens. Bioelectron. 21 (2005) 433–437.
[17] S. Lim, J. Wei, J. Lin, Q. Li, J. You, Biosens. Bioelectron. 20 (2005) 2341–2346.
[18] M.C. Daniel, D. Astruc, Chem. Rev. 104 (2004) 293–346.
[19] J. Li, Q. Yu, T. Peng, Anal. Sci. 21 (2005) 377–381.
[20] M. Yang, Y. Yang, H. Yang, G. Shen, R. Yu, Biomater. 27 (2006) 246–255.
[21] S. Qu, J. Wang, J. Kong, P. Yang, G. Chen, Talanta 71 (2007) 1096–1102.
[22] X.H. Kang, Z.B. Mai, X.Y. Zou, P.X. Cai, J.Y. Mo, J. Nanosci. Nanothech. 7 (2007) 1618–1619.
[23] K.B. Male, S. Hrapovic, Y. Liu, D. Wang, J.H.T. Luong, Anal. Chem. Acta 516 (2004) 35–41.
[24] S. Hrapovic, Y. Liu, K.B. Male, J.H.T. Luong, Anal. Chem. 76 (2004) 1083–1088.
[25] N. Zhu, Z. Chang, P. He, Y. Fang, Anal. Chim. Acta 545 (2005) 21–26.
[26] Y.C. Tsai, H.Y. Chien, J. Nanosci. Nanothech. 7 (2007) 1611–1617.
[27] Y. Wu, S. Hu, Colloids Surf. B: Biointerface 41 (2005) 299–304.
[28] M. Zhang, L. Su, L. Mao, Carbon 44 (2006) 276–283.
[29] X. Chu, D. Duan, G. Shen, R. Yu, Talanta 71 (2007) 2040–2047.
[30] K. Zhao, S. Zhuang, Z. Chang, H. Songm, L. Dai, P. He, Y. Fang, Electroanalysis 19 (2007) 1069–1074.
[31] L. Xu, Y. Zhu, L. Tang, X. Yang, C. Li, Electroanalysis 19 (2007) 717–722.
[32] H. Tang, J. Chen, S. Yao, L. Nie, G. Deng, Y. Kuang, Anal. Biochem. 331 (2004) 89–97.
[33] J. Ye, H. Cui, Y. Wen, W. Zhang, G. Xu, F. Sheu, Microchim. Acta 152 (2006) 267–275.
[34] L. Rong, C. Yang, Q. Qian, X. Xia, Talanta 72 (2007) 819–824.
[35] X.H. Kang, Z.B. Mai, X.Y. Zou, P.X. Cai, J.Y. Mo, Anal. Biochem. 363 (2007) 143–150.
[36] X. Luo, J. Xu, Q. Zhang, G. Yang, H. Chen, Biosens. Bioelectron. 21 (2005) 190–196.
[37] I. Gill, A. Ballesteros, Trend Biotech. 18 (2000) 282–296.
[38] T.M. Park, E.I. Iwuoha, M.R. Smyth, R. Freaney, A.J. McShane, Talanta 44 (1997) 973–978.
[39] A. Walcarius, D. Mandler, J.A. Cox, M. Collinson, O. Lev, J. Mater. Chem. 15 (2005) 3663–3689.
[40] X. Tan, Y. Tian, P. Cai, X. Zou, Anal. Bioanal. Chem. 381 (2005) 500–507.
[41] B. Wang, J. Zhang, G. Cheng, S. Dong, Anal. Chim. Acta 407 (2000) 111–118.
[42] H. Huang, Q. Yuan, X. Yang, Colloids Surf. B 39 (2004) 31–37.
[43] V. Radmilovic, H.A. Gasteiger, P.N. Ross, J. Catal. 154 (1995) 98–106.
[44] A.J. Bard, L.R. Faulkner, Electrochemical Methods Fundaments and Applied, John Willey and Sons Press, New York, 2000.
[45] R.A. Kamin, G.S. Willson, Anal. Chem. 52 (1980) 1198–1205.